J Nanopart Res (2015) 17:76
DOI 10.1007/s11051-015-2878-8

RESEARCH PAPER

Comparative evaluation of polymersome versus micelle structures as vehicles for the controlled release of drugs

Mona Alibolandi · Mohammad Ramezani · Khalil Abnous · Fatemeh Sadeghi · Farzin Hadizadeh

Received: 23 November 2014 / Accepted: 19 January 2015 / Published online: 6 February 2015

Abstract Di-block copolymers composed of two biocompatible polymers, poly(ethylene glycol) and poly(D,L-lactide), were synthesized by ring-opening polymerization for the preparation of doxorubicin-loaded self-assembled nanostructures, including polymeric vesicles (polymersomes) and micelles. The capability and stability of the nanostructures prepared for the controlled release of DOX are discussed in this paper. The in vitro drug release at 37 °C was evaluated up to 6 days at pH 7.4 and 5.5 and in the presence of 50 % FBS. The cellular uptake and cytotoxicity effect of both formulations were also evaluated in the MCF-7 cell line. The SEM and AFM images confirmed the hollow spherical structure of the polymersomes and the solid round structures of the micelles. The TEM results also revealed the uniformity in size and shape of the drug-loaded micelle and polymersome nanostructures. The DOX-loaded micelles and polymersomes presented efficient anticancer performance, as verified by flow cytometry and MTT assay tests. The most important finding of this study is that the prepared nanopolymersomes presented significant increases in the doxorubicin encapsulation efficiency and the stability of the formulation in comparison with the micelle formulation. In vitro studies revealed that polymersomes may be stable in the blood circulation and meet the requirements for an effective drug delivery system.

Keywords Micelles · Polymersomes · Di-block copolymer · Self-assembled · Doxorubicin · Nanomedicine

M. Alibolandi · F. Hadizadeh (✉)
Biotechnology Research Center, School of Pharmacy, Mashhad University of Medical Sciences, P.O. Box 9196773117, Mashhad, Iran
e-mail: hadizadehf@mums.ac.ir

M. Ramezani · K. Abnous
Pharmaceutical Research Center, School of Pharmacy, Mashhad University of Medical Sciences, Mashhad, Iran

F. Sadeghi (✉)
Targeted Drug Delivery Research Center, School of Pharmacy, Mashhad University of Medical Sciences, Mashhad, Iran
e-mail: sadeghif@mums.ac.ir

Introduction

The self-assembly of an amphiphile block copolymer in an aqueous environment is an attractive approach for fabricating nanoscale vesicular or micellar structures, which may present versatile properties in drug delivery and pharmaceutical applications.

The self-assembly phenomena of copolymers takes place based on different non-covalent interactions, including hydrophobic, hydrogen bindings or electrostatic interactions, the former of which are the major interactions involved in the self-assembly of amphiphilic block copolymers in aqueous solutions (Yan and Xie 2013).

The self-assembly of copolymers with various ratios of hydrophobic to hydrophilic blocks in the polymeric backbone was extensively investigated (Garofalo et al. 2014; Savoji et al. 2014; Savoji et al. 2013; Coupillaud et al. 2014).

An increase in the hydrophilicity of hydrophobe polymers via copolymerization with water-soluble hydrophilic polymers forces these copolymers to form polymeric vesicles (polymersomes) or micelle structures in aqueous solutions (Grubbs and Sun 2013; Mai and Eisenberg 2012; Letchford and Burt 2007).

It was previously shown that a hydrophilic volume fraction (f_{EO}) lower than 25 % in linear amphiphilic copolymers creates aggregates and solid particles, whereas values between 25 and 40 % induce polymeric vesicles (polymersomes), f_{EO} values in the range of 40–50 % result in hollow tubules and micelles are formed at f_{EO} values greater than 50 % (Discher et al. 1999).

Polymeric micelles and polymeric vesicles based on amphiphilic polymers have gained increasing interest as a drug vehicle and have vast applications in drug delivery (Brinkhuis et al. 2011; Lee et al. 2011; Li et al. 2014).

Polymer vesicles have unique properties, such as chemical stability, ability of encapsulating lipophilic drugs in their membranes or hydrophilic drugs in their interior aqueous compartment and tuneable surface functionalization (Meng and Zhong 2011).

Polymer micelles feature a lipophilic core that solubilizes hydrophobic drugs and a hydrophilic shell that make the entire assembly water-soluble (Yokoyama 2014). The ability of micelles to solubilize hydrophobic drugs expands the pharmaceutical potential of lipophilic drug molecules (Lebouille et al. 2013).

In the aforementioned drug delivery systems, hydrophobic drugs can be entrapped in the micellar core or the polymersome's shell through the use of various techniques, such as solution/precipitation, the salting-out process, film rehydration and the solvent evaporation method (Zhang et al. 2009; Zhan et al. 2010; Li et al. 2009; Jain and Kumar 2010; Li et al. 2007).

Polymeric vehicles based on amphiphilic copolymers of PEG and biodegradable polyesters can be used as a non-toxic, biodegradable and non-immunogenic system to solubilize drugs with low aqueous solubility (Xiao et al. 2010; Wang et al. 2012; Zhang et al. 2010).

The biological stability and reticuloendothelial system (RES) escape ability of the PEGylated polymeric nanoparticles after injection make them an ideal candidate for the delivery of therapeutic molecules (Gao et al. 2013).

The nanosize (<200 nm) of polymeric vehicles (micelles and polymersomes) causes the accumulation of anticancer drug-encapsulated particles at tumour sites due to the higher permeability of tumour blood vessels, leading to decreased side effects and an increase in the efficiency of cancer chemotherapy (Nahire et al. 2014; Jeetah et al. 2014).

In contrast, the nanosize of these particles can prevent renal excretion and enhance the escape of NPs from the RES (Kayser et al. 2005).

Drawbacks, such as the toxicity, short half-life and low solubility of hydrophobic anticancer drugs such as free base form of doxorubicin, docetaxel and paclitaxel in aqueous solution have hindered their application.

To overcome these obstacles, strategies such as the encapsulation of drugs into the polymeric particles have been attempted (Emami et al. 2014; Smejkalová et al. 2014; Cabral and Kataoka 2014; Colley et al. 2014; Xu et al. 2014). The employment of polymeric nanoparticles also provides an opportunity to tailor the release profiles of the encapsulated drugs (Palma et al. 2014; Gan et al. 2010).

For the encapsulation of drugs, polymeric micelles and polymeric vesicles offer several advantages, but a comparative study on the advantages of these systems has not yet been performed.

In this work, we evaluated the capability of the prepared PEG-PLA micelles and polymersomes as a doxorubicin drug delivery system through a series of tests, including the loading content, stability, in vitro release and cytotoxicity tests.

Materials and methods

Methoxy-PEG with a molecular weight of 5,000 Da, D,L-lactide and stannous octanoate (Tin(II) ethyl hexanoate) were purchased from Sigma Aldrich (Darmstadt, Germany). Doxorubicin hydrochloride was procured from Euroasia (New Delhi, India). The dialysis sac (cut off: 3.5 kDa) was purchased from Spectrum Labs (Darmstadt, Germany). All of the other chemical reagents and analytical-grade solvents were

obtained from Merck (Darmstadt, Germany) and were used as received.

Synthesis and purification of PEG-PLA copolymers

The synthesis of PEG-PLA copolymers was performed with two different block lengths of PEG-PLA, i.e. 5,000:5,000 (copolymer 1) and 5,000:15,000 (copolymer 2), by the ring-opening polymerization method.

The copolymers were synthesized under microwave irradiation. For example, to synthesize copolymer 1, 2.5 g of PEG_{5000} was introduced into a dry round-bottom flask equipped with a condenser, and the flask was then placed in a Milestone Microsynth microwave (Italy). The PEG was irradiated for 5 min at 1,000 W and 120 °C to increase the viscosity of the melted PEG. Then, 2 g of D,L-lactide and 10 μL of $Sn(Oct)_2$ were added to the dried viscous PEG, and the mixture was then irradiated and stirred at 1,000 W and 50 rpm at a constant temperature of 120 °C for 12 min. To purify the synthesized copolymer, the obtained copolymers were dissolved in an adequate amount of chloroform. The synthesized copolymers were then precipitated by the addition of excess (10-fold) cold diethyl ether. The purification process was repeated three times, and the precipitates were freeze-dried. The products were maintained at −20 °C until use.

Characterization of the PEG-PLA copolymers

The ^{1}H-NMR spectra of the PEG-PLA copolymers were recorded at room temperature using a Bruker Avance 400 MHz NMR spectrometer (Germany) in $CDCl_3$.

The ^{1}H NMR spectra were used to estimate the M_n of the copolymers from the integration ratio of the resonances at 5.4 ppm originating from the CH of the PLA block and at 3.8 ppm originating from the CH_2 of the ethylene glycol according to a previously established method (Jeong et al. 1999).

The molecular weights and polydispersity were determined using the Agilent GPC-Addon system and RID-A refractive index signal detector recording at 212 nm coupled to the PLgel columns and operated at a temperature of 25 °C. The molecular weights were calibrated with polystyrene standards. Tetrahydrofuran was used as the eluent (flow rate: 1 mL/min), and the sample injection volume was 10 μL.

Preparation of blank and drug-loaded nanoparticles

The PEG-PLA nanoparticles were prepared via the single emulsion solvent evaporation method.

The PEG-PLA copolymer with a predetermined concentration was dissolved in 1 mL of tetrahydrofuran, and the mixture was then added dropwise to deionized water to obtain a volume ratio of 1:5. The resulting solution was stirred for 6 h, and the organic solvent was evaporated under reduced pressure using a rotary evaporator to form the nanoparticles (NPs). Finally, the NPs were concentrated by ultrafiltration (30 min, 5,000 rpm, cut off: 30,000 Da).

The loading of DOX in the NPs was performed by neutralizing DOX-HCl with an equal molar amount of triethylamine (TEA) for 24 h in tetrahydrofuran (THF). The resulting solution was centrifuged at 3,000 rpm, and the resultant supernatant was filtered to obtain free DOX.

The appropriate amount of free DOX was added to the solution of 10 mg/mL PEG-PLA in THF under stirring. This solution was added dropwise to deionized water (1:5 ratios) under stirring at 1,200 rpm for 6 h, and the organic solvent was evaporated under reduced pressure using a rotary evaporator to form DOX-loaded NPs.

To remove the un-trapped DOX and TEA, the mixture was centrifuged and washed three times using ultrafiltration (30 min, 5,000 rpm, cut off: 30,000 Da). The suspension of nanoparticles was then freeze-dried using 2.5 % sucrose at −70 °C for 48 h (Lyotrap Plus, LTE Scientific Limited, UK) to obtain a spongy cake of the formulations.

Calculation of encapsulation efficiency and loading content

The amount of doxorubicin in the NPs was analysed by spectrophotometry measurements at $A = 480$ nm using a UV–Vis spectrophotometer (UV-160A Shimadzu, Japan). The doxorubicin-loaded nanoparticles were dissolved in dimethylsulfoxide (DMSO) at a concentration of 0.2 mg/mL, and the amount of DOX encapsulated in the polymersomes or micelles

structures was then calculated from the established standard curve.

The drug loading content (LC) and encapsulation efficiency (EE) of the prepared formulations were calculated using Eqs. 1 and 2, respectively.

$$\text{EE}\,\% = \text{Mass of drug loaded in NPs}/\text{Mass of drug initially used} \quad (1)$$

$$\text{LC}\,\% = \text{Mass of drug in the formulation}/\text{Mass of polymer in the formulation} \quad (2)$$

Physiochemical properties of self-assembled nanostructures

The measurement of the particles size and size distribution was performed by dynamic light scattering. Briefly, the particle suspensions were diluted 10 % in deionised water and then analysed with a Zetasizer (NANO-ZS, Malvern, UK) at a scattering angle of 90° equipped with a 4-mW He–Ne laser operated at 633 nm through back-scattering detection. All of the measurements were performed in triplicate at 25 ± 3 °C.

The morphologies of the blank micelles and polymersomes were examined with a JEOL-5300 scanning electron microscope (SEM) using an accelerating voltage of 100 kV.

Briefly, the freeze-dried NPs were mounted on stubs with colloidal graphite and sputter-coated with gold to an approximate thickness of 200 A° under vacuum for 5 min to prevent charging and distortion prior to SEM analysis.

An atomic force microscope (AFM, model: Nano Wizard®II NanoScience AFM, JPK Instruments Inc., Germany) was used to extensively evaluate the structures of these nanostructures. The sample for AFM analysis was prepared as follows: Microscope glass cover slips (24 × 24 mm^2, Fisher Scientific, UK) were washed with acetone and ethanol, rinsed with ultrapure filtered water and dried. After cleaning, the polymersomes or micelles were diluted in deionized water (0.5 mg/mL), dispensed onto the glass cover slips and dried at room temperature for 24 h. The measurements were performed in the tapping mode and dehydrated state in the air, and ACT cantilevers (JPK Instruments Inc., Germany) were used.

Transmission electron microscopy was performed to investigate the size and homogeneity of the prepared formulations using an electron microscope (HR-TEM; JEOL-2100) operated at 80 kV with a Gatan Orius SC600 CCD camera. The sample for TEM observation was prepared as follows: The suspension of NPs (0.5 mg/mL) was dropped onto copper grids coated with an amorphous carbon film and dried thoroughly in an electronic drying cabinet at a temperature of 25 °C and a relative humidity of 45 %.

Critical micelle concentration measurement

The critical micelle concentrations (CMCs) of the micelles and polymersomes in deionized water were determined using our modified dye solubilization method using iodine instead of pyrene (Khodaverdi et al. 2012).

A stock solution of iodine in acetone (12 mg/mL) was prepared. Aliquots of iodine (500 μL) were added to vials containing varied concentrations (2.5–0.009 mg) of polymers in 1 mL of deionized water and allowed to equilibrate for 48 h.

The absorbance of each sample was determined at 411 nm using a Synergy H4 Hybrid Multi-Mode Microplate Reader (Biotek, Model: H4MLFPTAD). An abrupt increase in the absorbance measurement indicated the formation of micelles.

In vitro drug release

The in vitro release of doxorubicin from the formulations was assessed by the dialysis method under sink condition. The doxorubicin-loaded formulation (1 mL) was introduced into a dialysis bag (MWCO 3.5 kDa) and then immersed into 50 mL of Phosphate Buffer Saline, PBS (0.1 M, pH 7.4), citrate buffer (0.1 M, pH 5.5) or PBS containing 50 % Foetal Bovine Serum (FBS) in a shaker incubator set at 90 rpm and 37 °C.

Samples (1 mL) were withdrawn at definite times and replaced by the addition of 1 mL of fresh release medium. The samples were analysed in a 96-well bottom black plate using a Synergy H4 Hybrid Multi-Mode Microplate Reader (Biotek, Model: H4MLFPTAD) with $\lambda_{excitation}$ and $\lambda_{emission}$ values set to 480 and 580 nm, respectively. All of the assays were performed in triplicate.

In vitro stability

The kinetic stability of the DOX-loaded micelles and polymersomes was evaluated in PBS pH 7.4 and 50 % FBS.

The DOX-loaded micelles or polymersomes (1 ml of 10 mg/mL suspension) were mixed with 1 mL of foetal bovine serum (100 %, Invitrogen), and the mixture was then incubated at 37 °C. At certain time intervals (0, 1, 3, 6, 12, 24 and 48 h), aliquots (100 μL) of the mixtures were withdrawn and analysed using dynamic light scattering.

The second experiment was performed to measure the scattered light intensity in PBS pH 7.4 at 37 °C.

The DOX-loaded micelle or polymersome solutions in PBS pH 7.4 (2 mL, concentration: 10 mg/mL) were also incubated at 37 °C, and at the same time intervals, the scattered light intensity was measured.

Storage condition of the formulations

The stability of the lyophilized doxorubicin-loaded micelles and polymersomes was evaluated after storage at −20, +4 and 25 °C for 6 months of storage. The particle size distribution and drug encapsulation efficiency of the samples were determined as a function of the storage time.

Cell culture

The MCF-7 (human breast carcinoma cell line) cells were obtained from the National Cell Bank of Iran, Pasteur Institute of Iran. The cells were maintained in RPMI 1640 medium (Gibco BRL, USA) supplemented with 10 % (v/v) heat-inactivated FBS (Gibco BRL, USA) and penicillin/streptomycin (100 U/mL, 100 units/mL) at 37 °C in a humidified atmosphere (95 %) containing 5 % CO_2.

Cytotoxicity studies

The cytotoxicity of DOX, blank or DOX-loaded micelles and polymersomes against MCF-7 cells was investigated using the MTT assay. The cells were seeded in 96-well plates at a density of 5,000 cells per well in 100 μL of RPMI 1640 with 10 % FBS (RPMI 1640 + FBS). After incubation for 24 h (37 °C, 5 % CO_2), the cells were treated with free DOX or DOX-loaded micelles or DOX-loaded nanopolymersomes in 100 μL of complete medium with 10 % FBS for 5 h (37 °C, 5 % CO). The medium was then removed, washed with PBS, replaced with fresh complete medium and further incubated for 48 h. After incubation for 48 h at 37 °C in a humidified incubator, 20 μL of MTT (5 mg/mL in PBS) was added to each well and incubated for 4 h. Then, MTT solution was aspirated from the wells using vacuum and 100 μL of DMSO was added to each well. After 20 min of mixing, the absorbance was recorded on a microplate reader at a wavelength of 545 nm with a reference wavelength of 630 nm.

Cellular uptake studies

Flow cytometry was also implemented to investigate the cellular uptake of the free DOX·HCl, blank or drug-loaded nanoparticles. The cells were plated in six-well plates at 1×10^5 cells/well and allowed to adhere overnight. The next day, the cells were incubated for 2 h with either free DOX·HCl or drug-loaded nanoparticles (DOX concentration: 20 μg/mL). The cells were then trypsinized, collected in complete media and centrifuged at 1,400 rpm for 10 min. The supernatants were removed, and the pellet was washed three times with PBS. The cells were then suspended in flow cytometry buffer (0.1 % sodium azide and 2 % FBS in PBS), and the intensity of the doxorubicin fluorescence in the cells was determined using a BD FACSCalibur equipped with a 488 laser in the FL2 channel. The data were analysed using the WinDMI 2.9 analysis software.

Data analysis

The results were reported as the mean ± SD ($n \geq 3$). The data were analysed by one-way analysis of variance (ANOVA). A probability value of less than 0.05 was considered significant.

Results and discussion

Synthesis and characterization of PEG-PLA copolymers

The two PEG-PLA copolymers were successfully synthesized by the ring-opening polymerization method.

The ^{1}HNMR spectra of the copolymers are shown in Fig. 1. The signal at 3.8 ppm is attributed to the methylene group of the PEG block in the copolymer chains. Its integral serves as an internal standard to calculate the average chain length of the PEG. The signal at 5.4 ppm is related to the CH of the lactide at the PLA block, and its integral can be used to estimate the average chain length of the PLA. The results of these analyses for two copolymers are summarized in Table 1.

Furthermore, Table 1 shows the molecular weight data resulting from the GPC analysis of the polymers after synthesis. The polydispersity of the copolymers indicates a narrow molecular weight distribution (<2) for all of the copolymers.

The GPC chromatogram of the synthesized copolymers is shown in Fig. 2. The unimodal and symmetrical GPC curve with a narrow molecular weight distribution verified the successful synthesis of the copolymers.

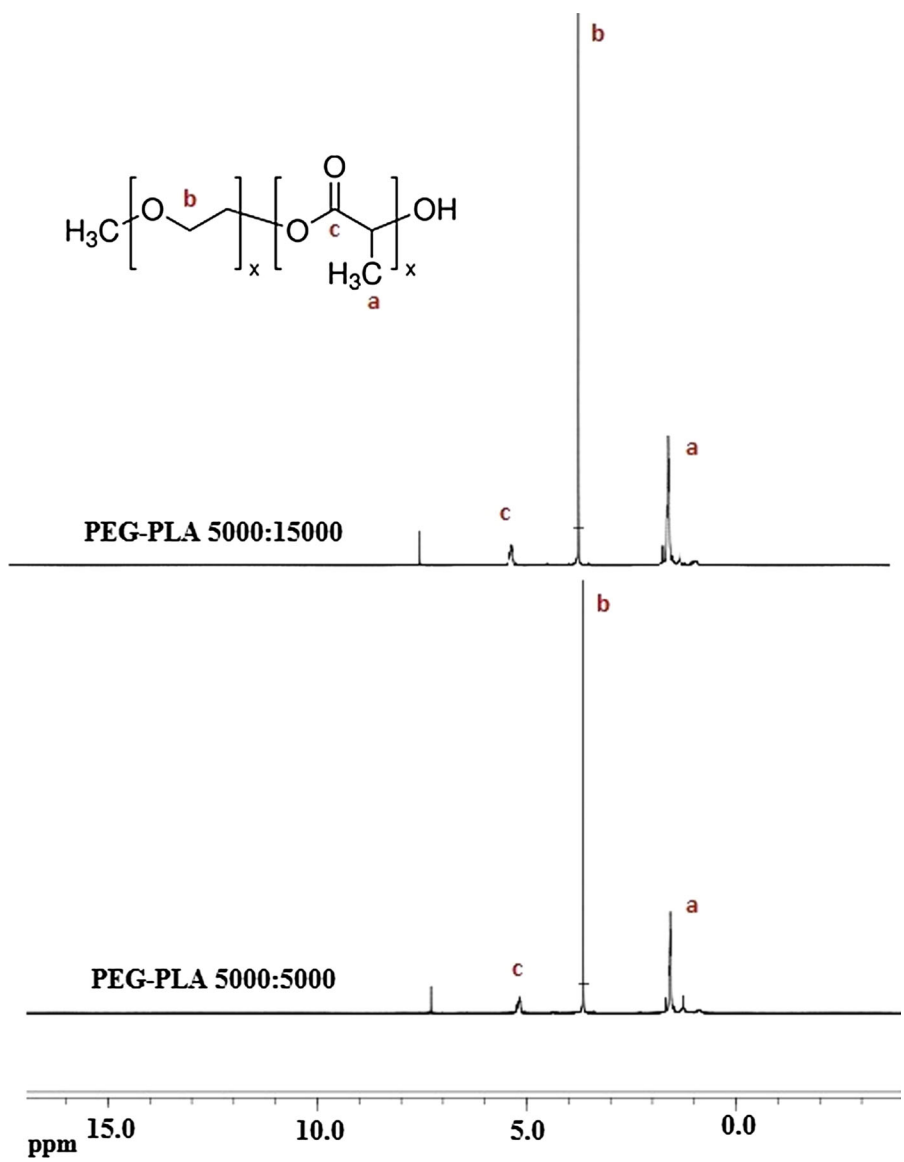

Fig. 1 ^{1}HNMR spectra of the synthesized copolymers

Table 1 Copolymer characteristics determined by ^{1}HNMR and GPC

	^{1}HNMR		GPC		
	M_w^a	PLA^b	M_n^c	M_w^d	M_w/M_n^e
PEG_5-PLA_5	8,589	3,589.68	7,872	9,027	1.14
PEG_5-PLA_{15}	18,654	13,654.12	11,265	18,250	1.62

[a] Molecular weight of copolymer determined by ^{1}HNMR

[b] Molecular weight of PLA block determined by ^{1}HNMR

[c] Number average molecular weight determined by GPC

[d] Average molecular weight determined by GPC

[e] Polydispersity determined by GPC

The results of polymer characterization tests confirm the efficacy of the microwave irradiation method for the synthesis of PEG-PLA copolymers.

The use of microwave irradiation in polymer science has become an interesting synthesis technique due to its unique advantages, such as the limited production of by-products, higher yield of polymerization reaction, easier scale up and short reaction times (Hoogenboom and Schubert 2007; Sosnik et al. 2011).

Preparation and characterization of NPs

Table 2 presents the sizes of the blank PEG-PLA nanoparticles produced through the single emulsion technique.

An increase in the hydrophobic segment resulted in an increase in the nanoparticle size due to the enhancement of hydrophobic interactions.

The PEG-PLA 5,000:5,000 copolymer formed micelles, which are tiny droplets created when the

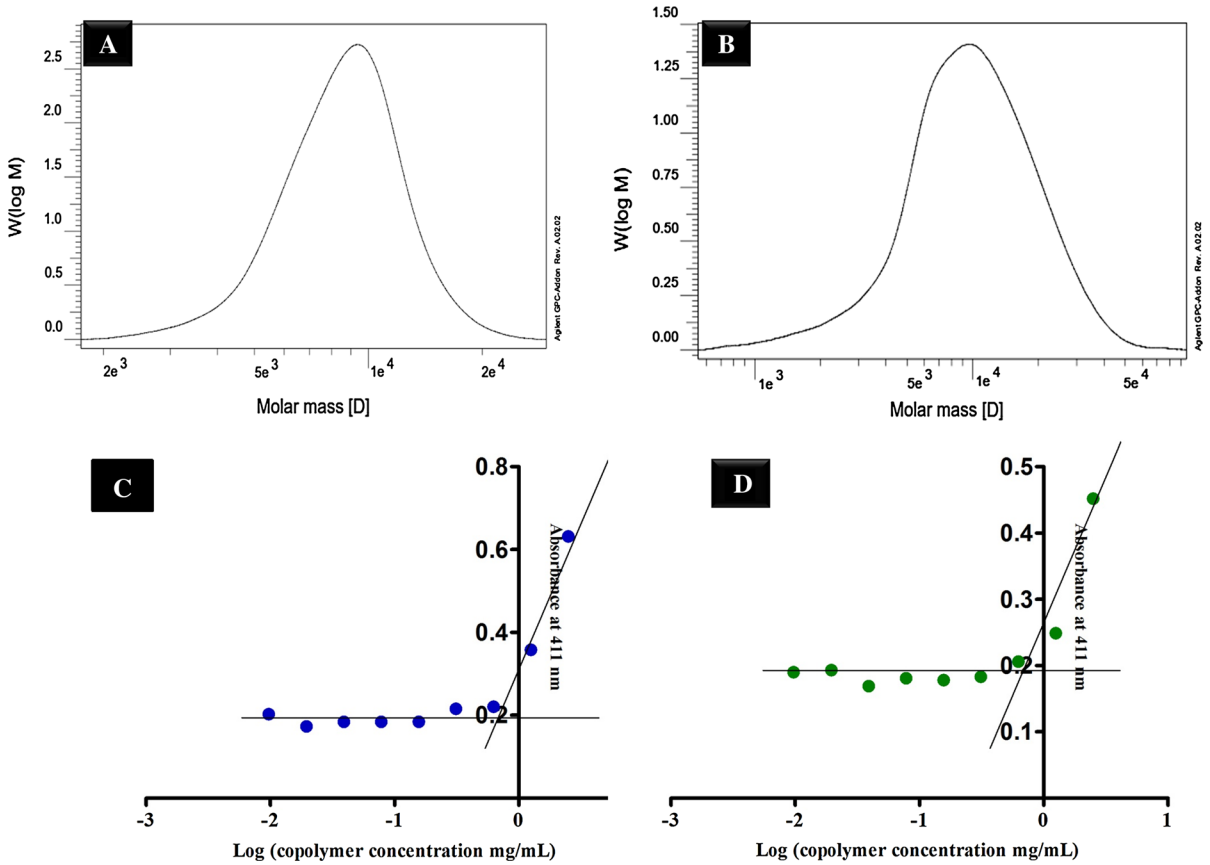

Fig. 2 GPC chromatogram of PEG5000-PLA5000 (**a**) and PEG5000-PLA15000 (**b**); Critical micelle concentration (CMC) of PEG5000-PLA5000 (**c**) and PEG5000-PLA15000 (**d**)

Table 2 Characteristics of blank polymersomes created by the single emulsion method

Copolymers	Z-average (nm)	PdI	Zeta potential (mV)
PEG_5-PLA_5	37.8 ± 3.27	0.21	−7.62
PEG_5-PLA_{15}	154.3 ± 1.64	0.162	−6.29

PEG segment of the copolymer faces the water and the PLA blocks are forced together away from the water.

However, in PEG-PLA 5000:15000, the hydrophobic PLA segment is too bulky to fit in the interior of a micelle, and the copolymer tends to form polymeric vesicles (polymersomes).

Due to the long hydrophobic chain length in PEG-PLA 5000:15000, they form a bilayer sheet. In this case, the PEG segments face the water molecules, and the hydrophobic PLA chains are oriented towards the inside of the bilayer. This copolymer created a vesicle structure in an aquatic environment.

The critical micelle concentrations (CMCs) of the polymers were then determined by plotting the intensity of the absorbance at 411 nm as a function of the logarithm of the concentrations. The CMC values of PEG5-PLA5 and PEG5-PLA15 are presented in Fig. 2c, d.

The low CMC values of the synthesized copolymers suggested that the micelles prepared from these copolymers are thermodynamically stable and can better maintain micellar integrity upon dilution.

The NPs were further studied by atomic force microscopy (AFM) in a dehydrated state.

As reported in Fig. 3b, the polymersomes exhibited "donutlike" structures with centres that are lower than their edges (height plot in Fig. 3d). This result indicates that the spheres observed by SEM and TEM are water-filled vesicles that will collapse into the dehydrated discs detected by AFM.

Figure 3d shows a sectional height profile of a donut and the lowest height is observed in the crater part.

The polymeric micelles were also attached to the surface of mica and remained tightly bound, as imaged with an AFM tip.

The shape of the polymeric micelles was typically observed to be single, smooth and round. The average diameter of the polymeric micelles was found to be 48 nm (Fig. 3a, c).

This superior nanoscale dimension enables these therapeutic carriers to prevent cellular uptake by the mononuclear phagocyte system (MPS), which introduces a major barrier in the drug delivery.

Furthermore, SEM was used to investigate the morphology of the polymersomes and micelles. Figure 4a shows a SEM image of the PEG-PLA 5000:15000 NPs, which demonstrates the hollow spherical configuration of the self-assembled polymersomes.

Figure 4b exhibits the SEM of the PEG-PLA 5000:5000 NPs, which demonstrates the small, solid (not hollow), round NPs.

The SEM image of the NPs also demonstrates that the sizes of the polymersomes and micelles were approximately 40 and 120 nm, respectively, which is consistent with the size measurement of DLS in Table 2.

Drug loading and in vitro drug release

Hydrophobic DOX was encapsulated into the core of the PEG-PLA micelles or the shells of the PEG-PLA polymersomes. The drug LC, EE and nanoparticle size are presented in Table 3.

The DOX-loaded polymersomes exhibited higher LC and EE in comparison with the micelles. The average sizes of the drug-loaded micelles were greater than that of the corresponding blank micelles. The sizes of the polymersomes were all approximately 152 nm, and this size is essentially related to the high capacity and structural stability of the nanopolymersomes after drug loading.

The configurations of the DOX-loaded polymersomes (P4) and DOX-loaded micelles (M4) are observed in Fig. 4a, b, respectively. Both formulations exhibited relatively mono-dispersed spherical nanoparticles, which make them ideal for further in vitro investigation.

The in vitro drug release profiles of all of the formulations were examined in PBS (pH 7.4 and pH 5.5) and PBS pH 7.4 containing 50 % FBS. The release rates of the polymersomes and micelles depended on the PEG/PLA ratios because the architecture of their corresponding self-assemblies was also different.

However, all of the release behaviours suggested that the release rate of DOX was higher at pH 5.5 than at pH 7.4, and PEG-PLA micelles exhibited higher release behaviour than the PEG-PLA polymersomes at the same pH.

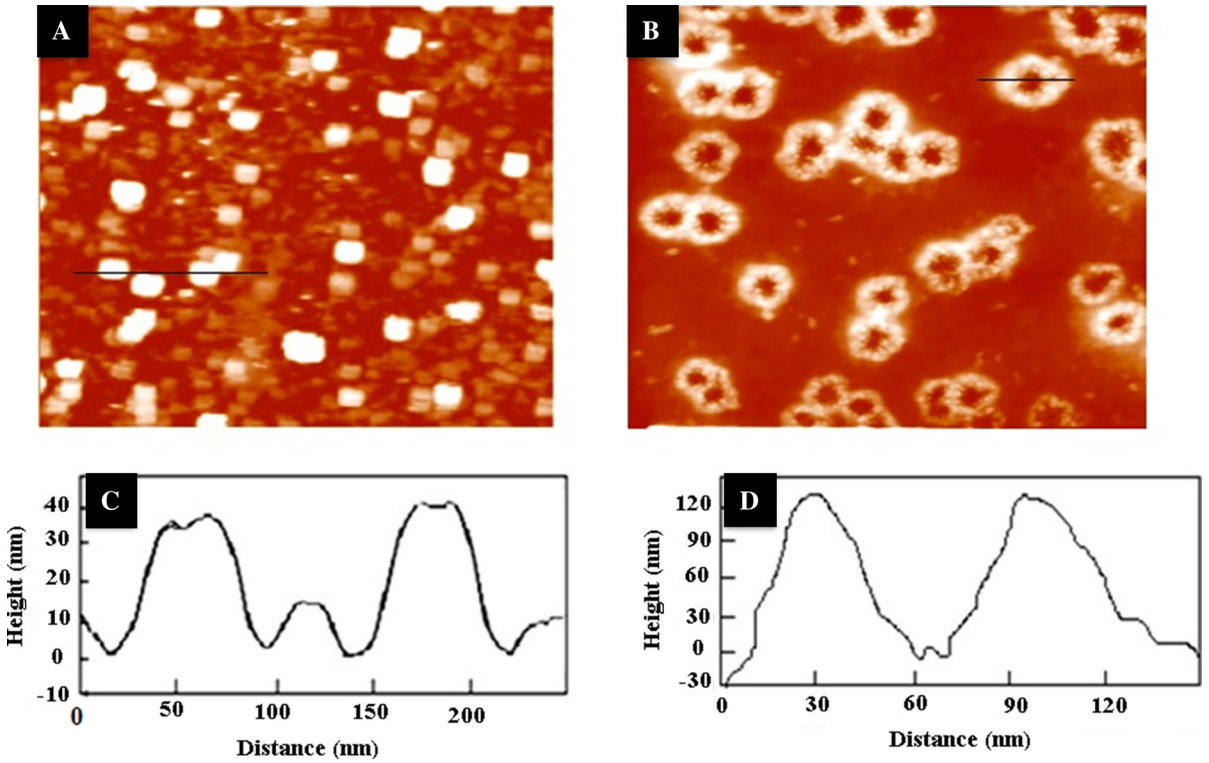

Fig. 3 AFM image of micelles (**a**) and polymersomes (**b**) obtained in the tapping mode. Height profile of micelles (**c**) and polymersomes (**d**)

To clarify this point, the DOX diffusion from micelles and polymersomes in pH 7.4 and 5.5 is shown in Fig. 5a, b, respectively. The release rates were accelerated in PBS at pH 5.5 due to the improved solubility of protonated DOX in water (Fig. 5b).

In fact, both the micelle and polymersome formulations exhibited an initial burst release in which the DOX release from the polymersome and micelle formulations was greater than 2 and 5 % within the 24 h. The burst release is related to the DOX adsorbed on the NP surface and/or to the release of the drug encapsulated near the NP surface (Magenheim et al. 1993). After this burst release, a constant DOX release was observed: after 7 days, approximately 4 and 8 % of the loaded drug were released from the polymersomes and micelles, showing a typical sustained and prolonged drug release that depends on drug diffusion and matrix erosion mechanisms (Fu and Kao 2010). The faster release profile of micelles may be a result of the accelerated destabilization of micelles due to the stronger hydrophilicity of their structures and the rapid penetration of water molecules and hydration of the NPs.

The polymersome formulation showed minimal DOX leakage in 50 % FBS (Fig. 6). In addition, more than 90 % of encapsulated DOX remained encapsulated, and no pronounced differences in the DOX release within 48 h were found between PBS pH 7.4 and PBS pH 7.4 containing 50 % FBS. In contrast, the micelles exhibited a slightly higher rate of release in 50 % FBS compared with PBS pH 7.4.

This result suggests that it takes time for doxorubicin to be released once encapsulated in the polymersome because polymeric bilayers are sufficiently stable to obtain a sustained release. Thus, a depot effect could be achieved using polymersomes (Ahmed and Discher 2004). The above results, which suggest that the drug would be stable in the blood circulation and released slowly at the tumour site, are indications that our polymersome formulation meets the requirements for an effective drug delivery system.

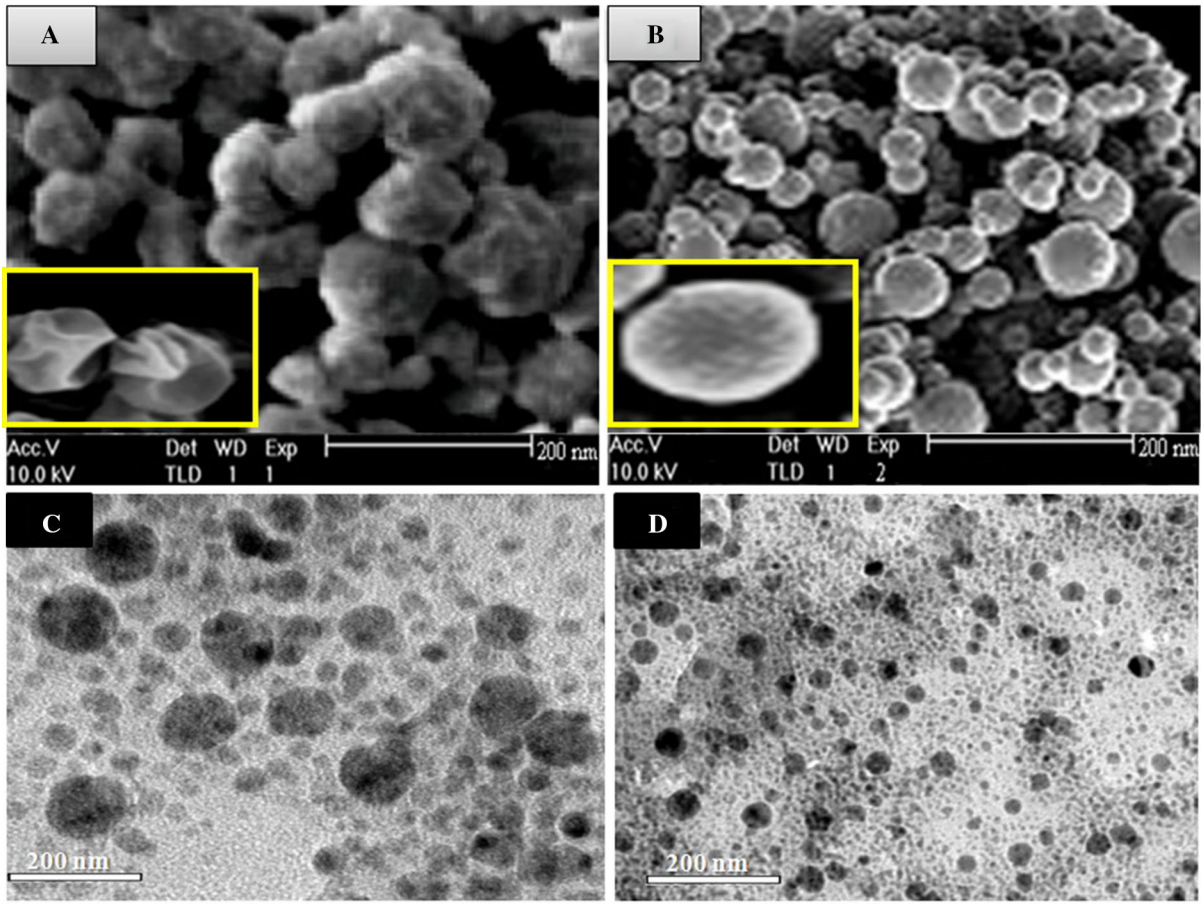

Fig. 4 SEM image of polymersomes (PEG5000-PLA15000) (**a**) and micelles (PEG5000-PLA5000) (**b**); TEM image of DOX-loaded polymersomes (**c**) and DOX-loaded micelles (**d**)

Table 3 Characteristics of DOX-loaded PEG-PLA micelles and polymersomes

Sample code	Copolymer	DOX (mg)	Polymer (mg)	LC %	EE %	Size (nm)	PDI
M1	PEG_5-PLA_5	0.1	10	0.951 ± 0.85	95.1 ± 0.43	42.6 ± 5.67	0.251
M2	PEG_5-PLA_5	0.25	10	2.33 ± 0.013	93.4 ± 0.32	44.1 ± 8.1	0.213
M3	PEG_5-PLA_5	0.5	10	3.37 ± 0.134	67.4 ± 2.68	46.2 ± 3.47	0.267
M4	PEG_5-PLA_5	1	10	6.561 ± 0.09	65.61 ± 0.9	51.8 ± 6.33	0.281
M5	PEG_5-PLA_5	2	10	11.04 ± 1.594	55.2 ± 7.97	98.7 ± 16.45	0.487
P1	PEG_5-PLA_{15}	0.1	10	0.986 ± 0.0015	98.63 ± 0.12	156.4 ± 1.23	0.121
P2	PEG_5-PLA_{15}	0.25	10	2.455 ± 0.033	98.2 ± 1.32	154.67 ± 3.11	0.113
P3	PEG_5-PLA_{15}	0.5	10	4.29 ± 0.413	85.8 ± 8.26	158.3 ± 2.69	0.192
P4	PEG_5-PLA_{15}	1	10	9.29 ± 0.438	92.9 ± 4.38	155.9 ± 3.74	0.127
P5	PEG_5-PLA_{15}	2	10	9.5 ± 0.604	47.5 ± 3.02	161.3 ± 1.94	0.178

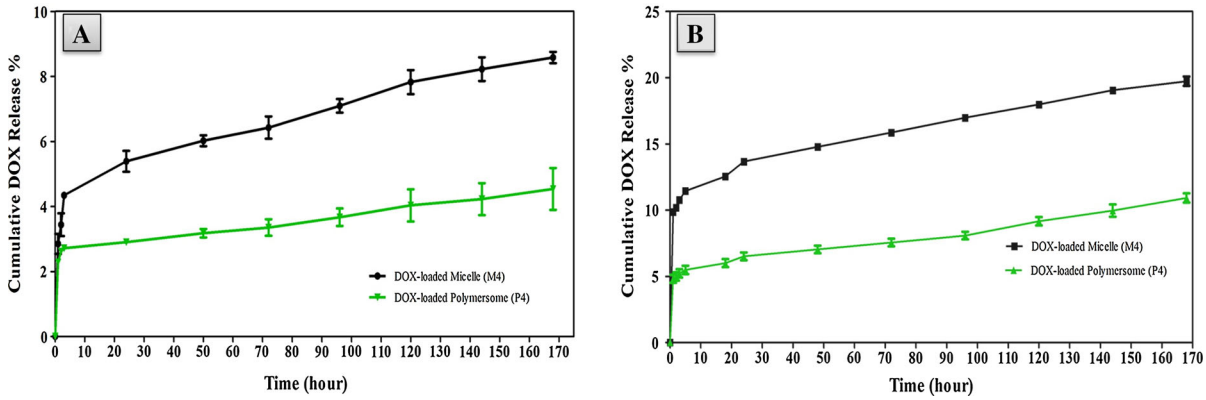

Fig. 5 Release profile of formulations P4 and M4 in PBS pH 7.4 (**a**) and citrate buffer pH 5.5 at 37 °C

Fig. 6 Release profile of formulations P4 and M4 in PBS pH 7.4 supplemented by FBS 50 % at 37 °C

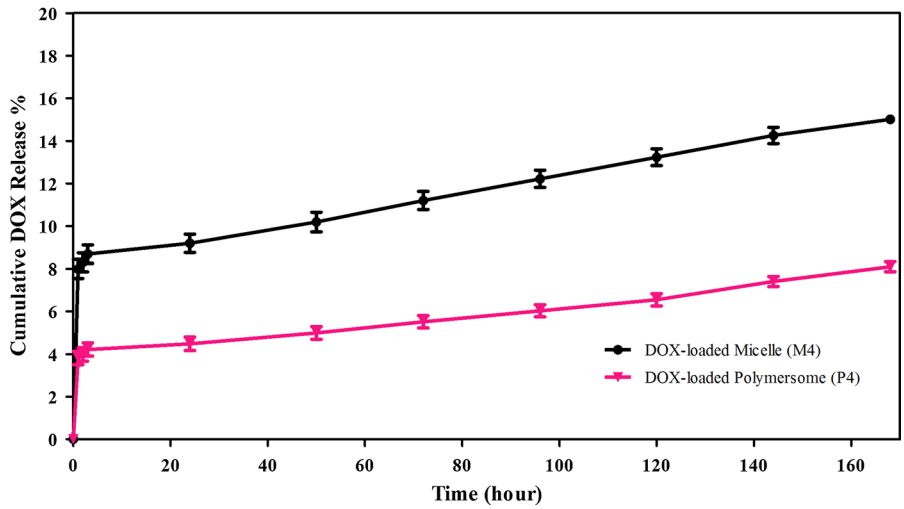

Stability kinetics

After intravenous injection, these self-assembled nanoparticles non-specifically interact with numerous proteins presents in plasma. These plasma proteins can absorb on the surfaces of micelles or polymersomes, which cause dissociation and aggregation of nanoparticles. To test the stability of the formulations, these DOX-loaded micelles and DOX-loaded polymersomes (1 mg/mL) were incubated with PBS pH 7.4 and 50 vol% FBS at 37 °C.

At different time intervals, the micelle solutions were analysed by DLS. Figure 7 shows the sizes and size distribution of DOX-loaded micelles and polymersomes at different time points in PBS pH 7.4 and 50 % FBS, respectively.

The incubation of DOX-loaded micelles in PBS revealed aggregation formation and marked changes in the size distribution pattern of micelles (Fig. 7a).

These findings suggest the sedimentation of micelles due to the formation of larger and denser particles as a result of water penetration and accelerated micelle hydration and consequently their instability. However, DOX-loaded polymersomes did not form any aggregation and size changes during incubation in PBS pH 7.4 because of their higher lipophilicity and bilayer stability (Fig. 7b).

In contrast, the co-incubation of both DOX-loaded micelles and polymersomes with FBS demonstrated changes in the size distribution pattern of micelles and polymersome after 6 and 48 h, respectively (Fig. 7c, d).

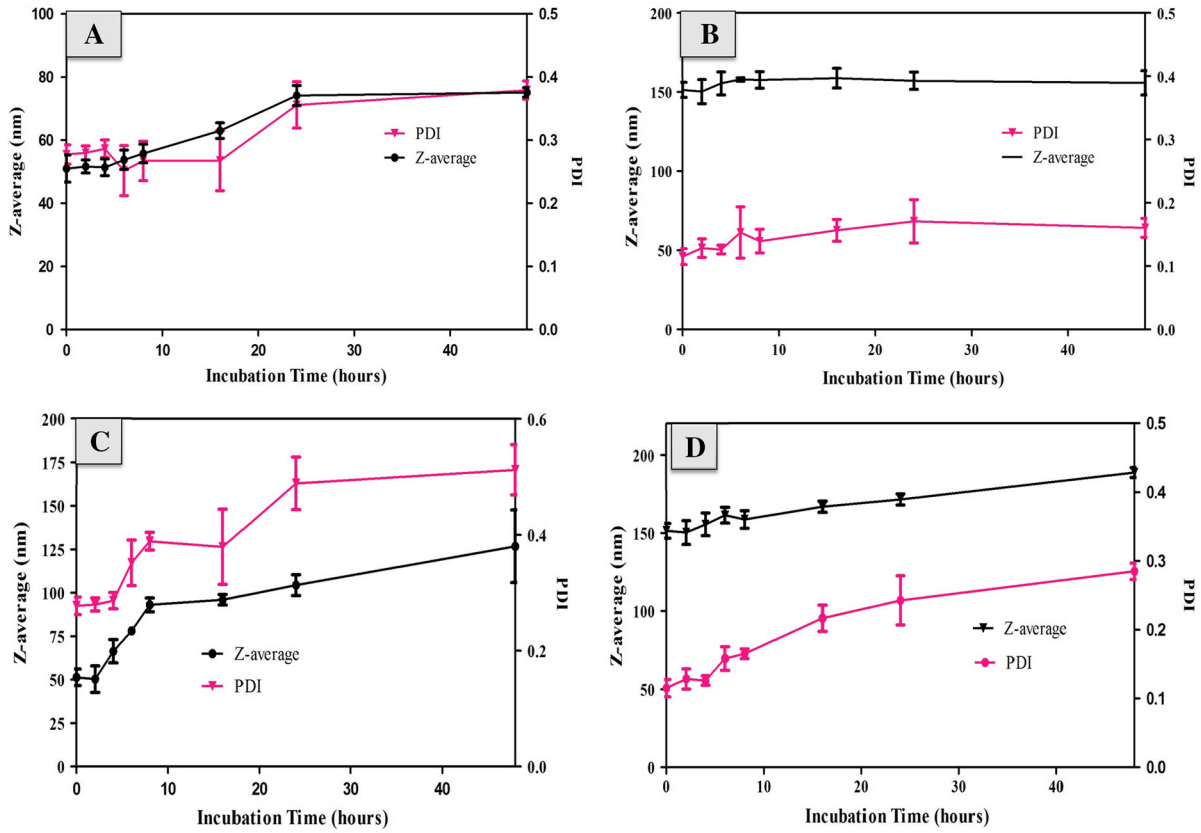

Fig. 7 Stability assessment of micelles (**a**) and polymersomes (**b**) in PBS pH 7.4 at 37 °C; Stability assessment of micelles (**c**) and polymersomes (**d**) in the presence of 50 % FBS at 37 °C

These findings suggest the sedimentation of micelles and polymersomes as a result of plasma protein adsorption in the presence of FBS proteins. However, polymersomes prepared from PEG-PLA 5000–15000 are more stable in FBS, as evident from their smaller and later change in the size and size distribution.

Because both NPs, including micelles and polymersomes, regardless of the same PEG outlayer, present PLA blocks with different lengths, this result highlights the importance of the PLA block length and self-assembly structure for improving the stability of NPs in serum-containing medium and the related opportunity to increase the NP half-life in the blood stream.

In this regard, the interaction between the PEG and plasma components was extensively investigated (Chen et al. 2008). Previously, the hydrogen bonding and van der Waals interactions between PEG and albumin were proven by Fourier transform infrared (FTIR) spectroscopy (Ragi et al. 2005) and binding force measurements, respectively (Rixman et al. 2003).

Moreover, the crystal structure analysis of PEG-protein complexes revealed electrostatic interactions between the PEG backbone and positively charged amino acids, including lysine, arginine and histidine (Hasek 2006). The formation of the PEG-protein complex likely induces NP aggregation and dissociation, which may cause the instability of NPs in vivo.

Storage condition

The powders of freeze-dried DOX-loaded micelle (M4) and DOX-loaded polymersome (P4) formulations were selected, and their shelf life time was evaluated at three different temperatures up to 6 months.

Initially, the mean diameter of NPs and EE % was 155.9 nm/92.9 % and 51.8 nm/65.6 % for P4 and M4, respectively.

No significant changes in the EE % were observed during the 6 months of storage for both formulations stored at −20 or 4 °C ($p > 0.05$), whereas there was a significant decrease in the EE % for the formulations stored at room temperature ($p < 0.05$).

The mean diameter of NPs showed an increase at all storage temperatures ($p < 0.05$), whereas the particle size of the formulations was increased after 6 months at room temperature. The results of the storage study are shown in Fig. 8.

Cytotoxicity of blank DOX-loaded micelles and polymersomes

The cytotoxicity of DOX-loaded micelles and polymersomes was evaluated against MCF7 cells in comparison with doxorubicin.

Figure 9a shows that the PEG-PLA copolymers do not have any significant cytotoxicity up to concentrations of 0.25–0.5 mg/ml.

Figure 9b shows the viability of MCF-7 cells after 48 h of incubation with free DOX-HCl, DOX-loaded micelles or polymersomes. The cells viability was concentration dependent. The IC_{50} value of DOX-loaded polymersomes is 3.84 μg/mL, which is greater than that of DOX-loaded micelles (1.63 μg/mL).

The lower potency of DOX-loaded polymersomes compared with DOX-loaded micelles can be ascribed to the slower release of DOX from more stable polymersomes structures, and similar observations have been reported from stability and release experiments.

The enhanced stability of polymersomes and their in vitro cytotoxicity suggest that DOX-loaded

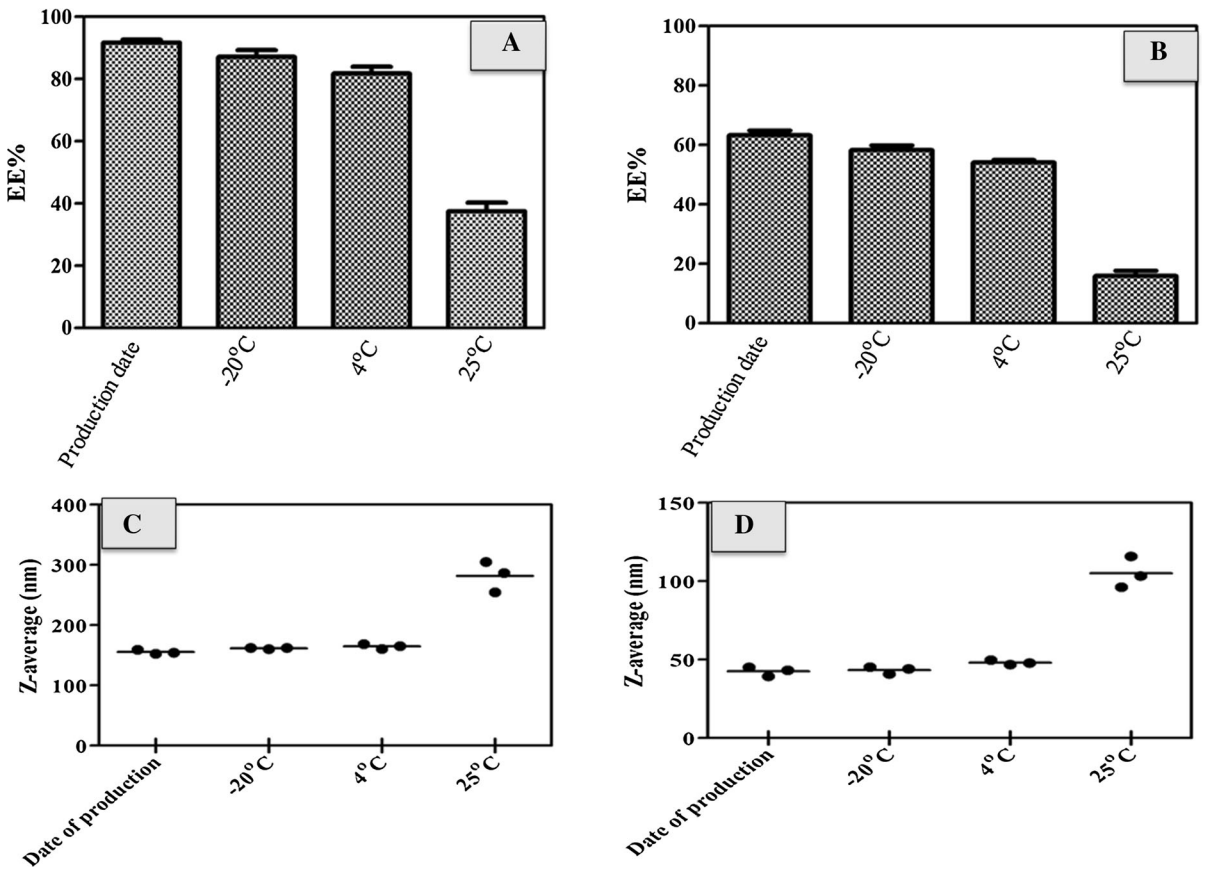

Fig. 8 Stability of lyophilized DOX-loaded micelles (**a**, **c**) and DOX-loaded polymersomes (**b**, **d**) after 6 months of storage at three different temperatures

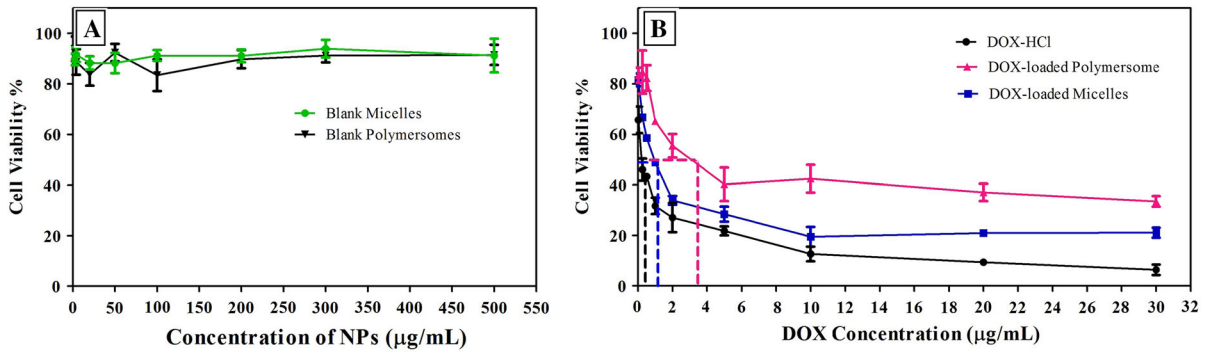

Fig. 9 Cytotoxicity of blank micelles and polymersomes on the MCF-7 cell *line* (**a**); Cytotoxicity of DOX-loaded micelles and DOX-loaded polymersomes on the MCF-7 cell *line* after 48 h (**b**)

polymersomes are a good candidate for the controlled delivery of DOX as a model of hydrophobic drugs.

Cellular uptake

To evaluate the cellular drug uptake behaviour of DOX-loaded micelles, DOX-loaded polymersomes and free DOX after incubation for 4 h, a flow cytometry analysis was performed.

It was observed that more DOX entered the cell than DOX-loaded micelles and DOX-loaded polymersomes.

The flow cytometry histograms prove that the DOX-encapsulated polymersomes exhibited less cellular uptake than the DOX-encapsulated micelles (Fig. 10). The obtained results provide evidence that the difference in the cytotoxicity of micelles and polymersomes obtained with the MTT assays originates from the greater stability of the polymersome structures and sustained release properties of this system in comparison with micelles. The faster destabilization of DOX-loaded micelles in the FBS-containing medium caused DOX leakage from the micelle cores. Consequently, the free DOX can be abundantly uptaken by cells.

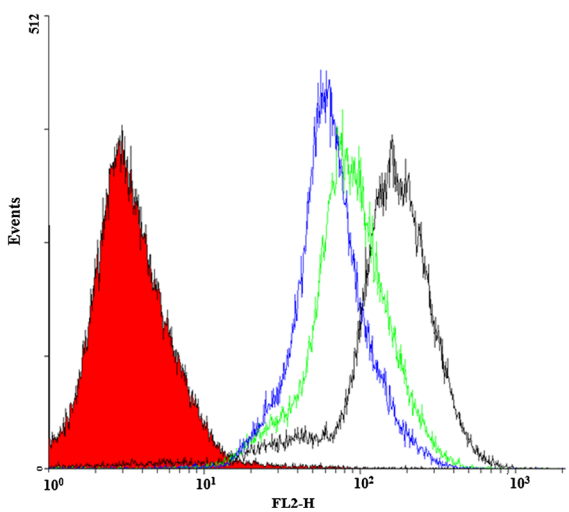

Fig. 10 Cellular uptake of free doxorubicin (*black line*), DOX-loaded micelles (*green line*) and DOX-loaded polymersomes (*blue line*) for 4 h at 37 °C. (Color figure online)

Conclusion

In this work, we present the synthesis and characterization of two amphiphilic block copolymers consisting of a hydrophilic PEG block (5,000 Da) and a poly(D,L-lactide) block with two different lengths (5,000 and 15,000 Da) using microwave-assisted ring-opening polymerization.

The PEG-PLA 5000–5000 and PEG-PLA 5000–15000 polymers form micelles and polymersomes, respectively, in an aquatic environment through a simple self-assembly process and can effectively encapsulate free base form of doxorubicin as a model of hydrophobic anticancer drugs.

As indicated by the stability study, micelles featuring more hydrophilic segments are thermodynamically less stable compared with polymersomes with a larger lipophilic segment.

As a result, a higher sustained release of DOX under simulated physiological conditions (pH 7.4, 37 °C) was observed with the polymersome formulation. These DOX-loaded micelles and polymersomes

showed dose-dependent cytotoxicity against the MCF-7 cell line, whereas the blank NPs exhibited minimal cytotoxicity. The current work highlights the capability of polymersomes in comparison with micelles for the sustained release of DOX as a model drug.

We proved the qualified properties of DOX-loaded polymersomes, their superior in vitro stability and their promising release characteristics compared with DOX-loaded micelles.

Acknowledgments The authors are grateful for the financial support provided by the Iran National Science Foundation (No. 9000719) and the Mashhad University of Medical Sciences (No. 901051). The authors would also like to thank Prof. Hossein Hosseinkhani from the National University of Taiwan for the valuable assistance provided.

Conflict of Interest The authors declare that they have no conflicts of interests.

References

Ahmed F, Discher DE (2004) Self-porating polymersomes of PEG-PLA and PEG-PCL: hydrolysis-triggered controlled release vesicles. J Control Release 96:37–53

Brinkhuis R, Rutjes FPJT, Hest JCM (2011) Polymeric vesicles in biomedical applications. Polym Chem 2:1449–1462

Cabral H, Kataoka K (2014) Progress of drug-loaded polymeric micelles into clinical studies. J Control Release 190: 465–476

Chen H, Kim S, He W et al (2008) Fast release of lipophilic agents from circulating PEG-PDLLA micelles revealed by in vivo forster resonance energy transfer imaging. Langmuir 24:5213–5217

Colley HE, Hearnden V, Avila-Olias M, Cecchin D, Canton I, Madsen J, MacNeil S, Warren N, Hu K, McKeating JA, Armes SP, Murdoch C, Thornhill MH, Battaglia G (2014) Polymersome-mediated delivery of combination anticancer therapy to head and neck cancer cells: 2D and 3D in vitro evaluation. Mol Pharm 11(4):1176–1188

Coupillaud P, Fèvre M, Wirotius AL, Aissou K, Fleury G, Debuigne A, Detrembleur C, Mecerreyes D, Vignolle J, Taton D (2014) Precision synthesis of poly(ionic liquid)-based block copolymers by cobalt-mediated radical polymerization and preliminary study of their self-assembling properties. Macromol Rapid Commun 35(4):422–430

Discher BM, Won YY, Ege DS, Lee JCM, Bates FS, Discher DE, Hammer DA (1999) Polymersomes: tough vesicles made from diblock copolymers. Science 284(5417):1143–1146

Emami J, Rezazadeh M, Rostami M, Hassanzadeh F, Sadeghi H, Mostafavi A, Minaiyan M, Lavasanifar A (2014) Co-delivery of paclitaxel and α-tocopherol succinate by novel chitosan-based polymeric micelles for improving micellar stability and efficacious combination therapy. Drug Dev Ind Pharm 14:1–11

Fu Y, Kao WJ (2010) Drug release kinetics and transport mechanisms of non-degradable and degradable polymeric delivery systems. Expert Opin Drug Deliv 7(4):429–444

Gan CW, Chien S, Feng SS (2010) Nanomedicine: enhancement of chemotherapeutical efficacy of docetaxel by using a biodegradable nanoparticle formulation. Curr Pharm Des 16(21):2308–2320

Gao H, Liu J, Yang C, Cheng T, Chu L, Xu H, Meng A, Fan S, Shi L, Liu J (2013) The impact of PEGylation patterns on the in vivo biodistribution of mixed shell micelles. Int J Nanomed 8:4229–4246

Garofalo C, Capuano G, Sottile R, Tallerico R, Adami R, Reverchon E, Carbone E, Izzo L, Pappalardo D (2014) Different insight into amphiphilic PEG-PLA copolymers: influence of macromolecular architecture on the micelle formation and cellular uptake. Biomacromolecules 15(1): 403–415

Grubbs RB, Sun Z (2013) Shape changing polymer assemblies. Chem Soc Rev 42(17):7436–7445

Hasek J (2006) Poly(ethylene glycol) interactions with proteins. Z Kristallogr (suppl 23): 613–618

Hoogenboom R, Schubert US (2007) Microwave-assisted polymer synthesis: recent developments in a rapidly expanding field of research. Macromol Rapid Commun 28(4):368–386

Jain JP, Kumar N (2010) Development of amphotericin B loaded polymersomes based on $(PEG)_3$-PLA co-polymers: factors affecting size and in vitro evaluation. Eur J Pharm Sci 40(5):456–465

Jeetah R, Bhaw-Luximon A, Jhurry D (2014) Polymeric nanomicelles for sustained delivery of anti-cancer drugs. Mutat Res, Fundam Mol Mech Mutagen 768:47–59

Jeong B, Choi YK, Bae YH, Zentner G, Kim SW (1999) New biodegradable polymers for injectable drug delivery systems. J Control Release 62(1–2):109–114

Kayser O, Lemke A, Hernández-Trejo N (2005) The impact of nanobiotechnology on the development of new drug delivery systems. Curr Pharm Biotechnol 6(1):3–5

Khodaverdi E, Tekie FS, Mohajeri SA, Ganji F, Zohuri G, Hadizadeh F (2012) Preparation and investigation of sustained drug delivery systems using an injectable, thermosensitive, in situ forming hydrogel composed of PLGA-PEG-PLGA. AAPS PharmSciTech 13(2):590–600

Lebouille JG, Vleugels LF, Dias AA, Leermakers FA, Cohen Stuart MA, Tuinier R (2013) Controlled block copolymer micelle formation for encapsulation of hydrophobic ingredients. Eur Phys J E Soft Matter 36(9):9919

Lee JS, Ankone M, Pieters E, Schiffelers RM, Hennink WE, Feijen J (2011) Circulation kinetics and biodistribution of dual-labeled polymersomes with modulated surface charge in tumor-bearing mice: comparison with stealth liposomes. J Control Release 155:282–288

Letchford K, Burt H (2007) A review of the formation and classification of amphiphilic block copolymer nanoparticulate structures: micelles, nanospheres, nanocapsules and polymersomes. Eur J Pharm Biopharm 65(3):259–269

Li S, Byrne B, Welsh J, Palmer AF (2007) Self-assembled poly(butadiene)-b-poly(ethylene oxide) polymersomes as paclitaxel carriers. Biotechnol Prog 23(1):278–285

Li Y, Qi XR, Maitani Y, Nagai T (2009) PEG-PLA diblock copolymer micelle-like nanoparticles as all-trans-retinoic

acid carrier: in vitro and in vivo characterizations. Nanotechnology 20(5):055106

Li S, Wu W, Xiu K, Xu F, Li Z, Li J (2014) Doxorubicin loaded pH-responsive micelles capable of rapid intracellular drug release for potential tumor therapy. J Biomed Nanotechnol 10(8):1480–1489

Magenheim B, Levy MY, Benita S (1993) A new in vitro technique for evaluation of drug release profile from colloidal carriers-ultrafiltration technique at low pressure. Int J Pharm 94:115–123

Mai Y, Eisenberg A (2012) Self-assembly of block copolymers. Chem Soc Rev 41(18):5969–5985

Meng F, Zhong Z (2011) Polymersomes spanning from nano- to microscales: advanced vehicles for controlled drug delivery and robust vesicles for virus and cell mimicking. J Phys Chem Lett 2:1533–1539

Nahire R, Haldar MK, Paul S, Ambre AH, Meghnani V, Layek B, Katti KS, Gange KN, Singh J, Sarkar K, Mallik S (2014) Multifunctional polymersomes for cytosolic delivery of gemcitabine and doxorubicin to cancer cells. Biomaterials 35(24):6482–6497

Palma G, Conte C, Barbieri A, Bimonte S, Luciano A, Rea D, Ungaro F, Tirino P, Quaglia F, Arra C (2014) Antitumor activity of PEGylated biodegradable nanoparticles for sustained release of docetaxel in triple-negative breast cancer. Int J Pharm 473(1–2):55–63

Ragi C, Sedaghat-Herati MR, Ouameur AA, Tajmir-Riahi HA (2005) The effects of poly(ethylene glycol) on the solution structure of human serum albumin. Biopolymers 78: 231–236

Rixman MA, Dean D, Ortiz C (2003) Nanoscale intermolecular interactions between human serum albumin and low grafting density surfaces of poly(ethylene oxide). Langmuir 19:9357–9372

Savoji MT, Strandman S, Zhu XX (2013) Switchable vesicles formed by diblock random copolymers with tunable pH- and thermo-responsiveness. Langmuir 29(23):6823–6832

Savoji MT, Strandman S, Zhu XX (2014) Invertible vesicles and micelles formed by dually-responsive diblock random copolymers in aqueous solutions. Soft Matter 10(32): 5886–5893

Smejkalová D, Nešporová K, Hermannová M, Huerta-Angeles G, Cožíková D, Vištejnová L, Safránková B, Novotný J, Kučerík J, Velebný V (2014) Paclitaxel isomerisation in polymeric micelles based on hydrophobized hyaluronic acid. Int J Pharm 466(1–2):147–155

Sosnik A, Gotelli G, Abraham GA (2011) Microwave-assisted polymer synthesis (MAPS) as a tool in biomaterials science: how new and how powerful. Prog Polym Sci 36(8):1050–1078

Wang R, Xiao R, Zeng Z, Xu L, Wang J (2012) Application of poly(ethylene glycol)-distearoylphosphatidylethanolamine (PEG-DSPE) block copolymers and their derivatives as nanomaterials in drug delivery. Int J Nanomed 7:4185–4198

Xiao RZ, Zeng ZW, Zhou GL, Wang JJ, Li FZ, Wang AM (2010) Recent advances in PEG-PLA block copolymer nanoparticles. Int J Nanomed 5:1057–1065

Xu J, Zhao Q, Jin Y, Qiu L (2014) High loading of hydrophilic/hydrophobic doxorubicin into polyphosphazene polymersome for breast cancer therapy. Nanomedicine 10(2):349–358

Yan LT, Xie XM (2013) Computational modeling and simulation of nanoparticle self-assembly in polymeric systems: Structures, properties and external field effects. Prog Polym Sci 38(2):369–405

Yokoyama M (2014) Polymeric micelles as drug carriers: their lights and shadows. J Drug Target 22(7):576–583

Zhan C, Gu B, Xie C, Li J, Liu Y, Lu W (2010) Cyclic RGD conjugated poly(ethylene glycol)-co-poly(lactic acid) micelle enhances paclitaxel anti-glioblastoma effect. J Control Release 143(1):136–142

Zhang H, Xia H, Wang J, Li Y (2009) High intensity focused ultrasound-responsive release behavior of PLA-b-PEG copolymer micelles. J Control Release 139(1):31–39

Zhang W, Li Y, Liu L, Sun Q, Shuai X, Zhu W, Chen Y (2010) Amphiphilic toothbrushlike copolymers based on poly(ethylene glycol) and poly(epsilon-caprolactone) as drug carriers with enhanced properties. Biomacromolecules 11(5):1331–1338